

Mechanism of Jet-Flutter : Self-Induced Oscillation of an Upward Plane Jet Impinging on a Free Surface*

Haruki MADARAME** and Masao IIDA***

An upward plane jet impinging on the free surface of a shallow rectangular tank oscillates without any external periodic force. The movement of the impinging point leaves additional fluid mass on the surface behind the point, which does not balance the momentum supplied by the jet. The imbalance generates propagating waves, and a surface level gap appears there. The level gap is flattened not by the waves but by the vertical motion of water columns. The imbalance causes lateral displacement of jet, which in turn causes the imbalance, forming a positive feedback loop. The above model explains well why the frequency corresponds to that of water column oscillation in a partitioned tank with the same water depth, and the oscillation region has a wide range above a certain velocity limit determined by the water depth.

Key Words: Flow-Induced Vibration, Plane Jet, Water Column Oscillation, Free Surface, Self-Excited Vibration, Energy Supply Mechanism

1. Introduction

Two types of self-induced oscillations are observed in a rectangular tank where an upward plane jet is issued from the bottom center: self-induced sloshing⁽¹⁾ and jet-flutter⁽²⁾. There remain two unsolved problems concerning jet-flutter, which is a transverse oscillation of a submerged upward plane water jet impinging directly on the free surface: why the frequency corresponds to that of water column oscillation in a partitioned tank with the same water depth, and why it occurs above a certain velocity limit determined by the water depth. Self-induced oscillation requires a chain of events that constitute a feedback loop. In this paper, the effect of transverse displacement of jet on oscillation is discussed, then the behavior of a jet receiving periodic transverse force is calculated using a simplified method and is verified by

experiment. Finally, the oscillation region estimated by the feedback loop model is compared with that determined by experiment.

2. Characteristics of Phenomenon

When an upward plane water jet at the center of a rectangular tank impinges on a free surface and

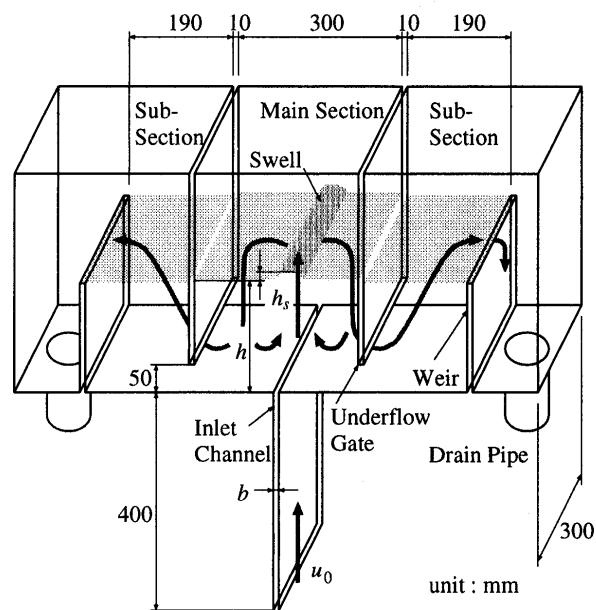


Fig. 1 Test tank

* Received 8th January, 1998. Japanese original: Trans. Jpn. Soc. Mech. Eng., Vol. 63, No. 612, B (1997), p. 2739-2744 (Received 17th October, 1996)

** Nuclear Engineering Research Laboratory, University of Tokyo, 2-22 Shirakata-Shirane, Tokai-mura, Ibaraki 319-1106, Japan

*** O-arai Engineering Center, Power Reactor and Nuclear Fuel Development Corporation, 4002 Narita-machi, O-arai-machi, Ibaraki 311-1313, Japan

makes a swell as shown in Fig. 1, the swell oscillates in the direction of jet thickness and is accompanied by an alternate level oscillation of the surfaces divided by the swell ridge. The frequency is well approximated by the following equation as shown in Fig. 2.

$$\omega = \sqrt{\frac{g}{h + h_s/2}} \quad (1)$$

where g is the acceleration due to gravity, and h is the distance from the jet inlet to the surface. The jet inlet is placed at the tank bottom in this study; therefore, h corresponds to the water depth. Equation (1) denotes the frequency of water column oscillation in connected tanks, where the increase in column height due to swell height of h_s is taken into account. Jet-flutter occurs in a wide range of jet velocities above a certain limit, and the velocity limit depends on h as shown in Fig. 3. The limit depends also on the jet inlet thickness b ; the limit decreases with increasing jet thickness. When the tank is deep ($h > 0.2$ m), jet impingement does not make an obvious swell anymore. The first-mode sloshing was induced in the

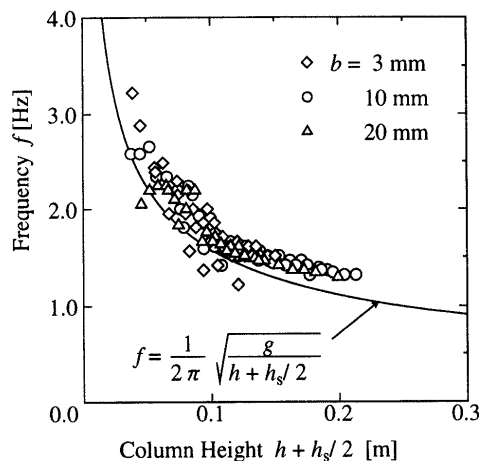


Fig. 2 Frequency

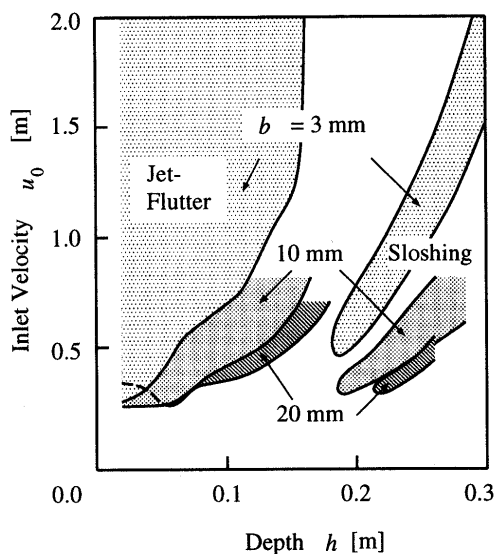


Fig. 3 Oscillation region

tank under a certain condition⁽¹⁾. In this paper, we discuss the mechanism of only the jet-flutter, not self-induced sloshing.

3. Surface Level Gap Formation Due to Swell Movement

Since gravity balances not with pressure gradient but with the deceleration of water in the swell, the pressure beneath the swell is not necessarily higher than that in the surroundings. Isobaric lines projecting toward the free surface are still symmetric with respect to the jet centerline. When the swell-making jet moves laterally, water having upward momentum is supplied to the swell at the front, and is decelerated at the rear. There appears an imbalance of pressure: low pressure at the front and high pressure at the rear. In the following, let the origin be the jet inlet, the y -axis be the horizontal direction and the x -axis be the vertical direction as shown in Fig. 4. The central position of jet η_h moves with velocity $d\eta_h/dt$ without changing the velocity profile $f(y - \eta_h)$. If the imbalance appears immediately after the movement, the generation of imbalance can be expressed using the derivative of f as follows.

$$q(t, y) = f'(y - \eta_h) \frac{d\eta_h}{dt} \quad (2)$$

Consider an infinitesimally thin jet of the velocity profile $\delta(y - \eta_h)$ moving laterally at a speed of $d\eta_h/dt$, where δ is Dirac's delta function. Water loses momentum u_h/g after being projected from the surface with velocity u_h . Taking the delay into consideration, the generation of imbalance can be expressed as

$$q(t', y) = \frac{u_h^2}{2g} \delta'(y - \eta_h(t' - \frac{u_h}{g})) \frac{d\eta_h}{dt} \Big|_{t' - u_h/g} \quad (3)$$

where δ' is the derivative of Dirac's delta function. The imbalance splits in two: one is propagated in the positive y -direction, the other in the negative direction with wave velocity c . The wave height is

$$\zeta^+(t, y) = -\frac{u_h^2}{4gc} \delta(y - ct + ct') \frac{d\eta_h}{dt} \Big|_{t' - u_h/g} \quad (4)$$

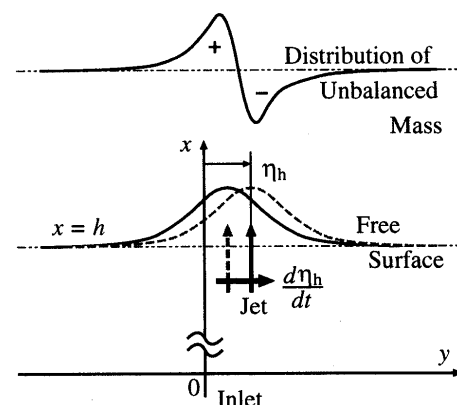


Fig. 4 Moving jet and swell

at $y > 0$, and

$$\zeta^-(t, y) = \frac{u_h^2}{4gc} \delta(y + ct - ct') \frac{d\eta_h}{dt} \Big|_{t' = u_h/g} \quad (5)$$

at $y < 0$. It should be noted that the wave height at $y < 0$ is opposite to that at $y > 0$. Let us consider the following oscillation of η_h .

$$\eta_h = Y \cos \omega t \quad (6)$$

The oscillation continuously generates the imbalance. The resultant wave height is as follows.

$$\zeta^+(t, y) = \frac{\omega^2 Y u_h^2}{4gc^2} \sin \omega \left(t - \frac{y}{c} - \frac{u_h}{g} \right) \quad (y > 0) \quad (7)$$

$$\zeta^-(t, y) = -\frac{\omega^2 Y u_h^2}{4gc^2} \sin \omega \left(t + \frac{y}{c} - \frac{u_h}{g} \right) \quad (y < 0) \quad (8)$$

Equations (7) and (8) are not continuous at $y = 0$ as shown in Fig. 5.

If the jet is not infinitesimally thin and has a velocity profile of $f(y - \eta_h)$, the wave height can be calculated as follows.

$$\zeta = \frac{\omega^2 Y}{4gc^2} \left\{ \int_{-\infty}^y f^2(y') \sin \omega \left(t - \frac{y}{c} - \frac{f(y')}{g} \right) dy' - \int_y^{\infty} f^2(y') \sin \omega \left(t + \frac{y}{c} - \frac{f(y')}{g} \right) dy' \right\} \quad (9)$$

The above results in a continuous surface form as shown in Fig. 6, but the level change at $y = 0$ is still

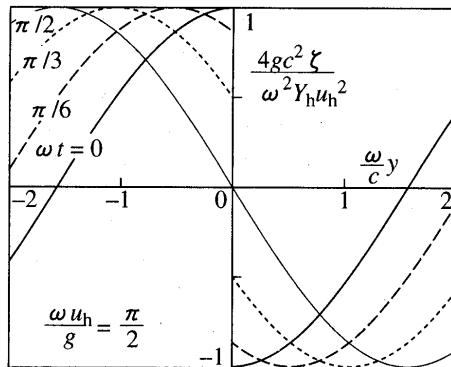


Fig. 5 Generation of level difference by extremely thin jet

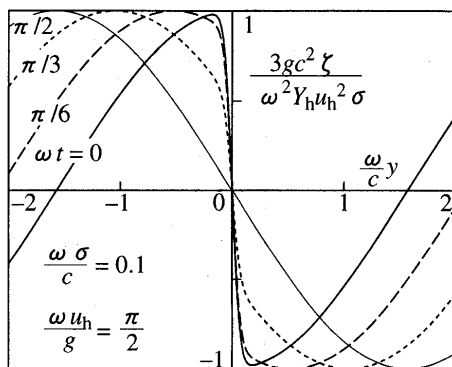


Fig. 6 Generation of level difference by jet of finite thickness

very steep. Equations (7) and (8) are a good approximation of Eq. (9).

The surface level gap exists after the propagation of waves. It cannot generate additional waves propagating in the y -direction to lessen itself. It seems as if there exists a wall at $y = 0$ through which no water passes. Since the wavelength is fairly large, the water level can be regarded as flat on either side. The level difference near $y = 0$ can be expressed as follows.

$$\zeta = \pm \frac{\omega^2 Y u_h^2 \Delta y}{4gc^2} \sin \omega \left(t - \frac{u_h}{g} \right), \quad (10)$$

where Δy is the thickness of the jet.

4. Mechanism Governing Frequency

Although the surface level gap does not generate waves in the y -direction, it can induce water motion in the x -direction. Consider two water columns: one from the jet inlet to the free surface on $y > 0$ side, and the other to the surface on $y < 0$. The gravitational force is proportional to the water level, while they have the same pressure difference between the bottom and the free surface. Thus the columns are accelerated as follows.

$$L \frac{d^2 \zeta}{dt^2} = -g \zeta, \quad (11)$$

where L is the average column height and ζ is the level fluctuation. The equation of oscillation, Eq. (11), gives a natural frequency of $\omega = \sqrt{g/L}$. The column height including half of the swell height is $h + h_s/2$; thus, we conclude that the frequency is given by Eq. (1). Since there is a phase difference of 180° between the two columns, acceleration is canceled out near the jet inlet. Water near the inlet does not oscillate at all, the x -directional motion occurs only near the surface, and the frequency is still $\sqrt{g/L}$.

5. Energy Supply to Oscillation

Consider the following water column oscillation.

$$\zeta = \pm X \cos \omega t, \quad (12)$$

where the sign is positive at $y > 0$. The pressure difference across the jet is

$$\Delta p = 2\rho g X \cos \omega t, \quad (13)$$

where ρ is the density of water. The pressure difference is uniform in the x -direction. Let us assume that the lateral displacement of jet on the surface η_h can be expressed by the following equation.

$$\eta_h = -\varepsilon_1 X \cos(\omega t - \phi_1), \quad (14)$$

where ε_1 is amplification factor and ϕ_1 is phase lag. The oscillation of η_h generates a level difference expressed by Eq. (10), which induces the following vertical force.

$$F = \pm \varepsilon_1 \varepsilon_2 X \sin(\omega t - \phi_1 - \phi_2), \quad (15)$$

where $\varepsilon_2 = \rho \omega^2 u_h^2 \Delta y / 4c^2$ and $\phi_2 = \omega u_h / g$. The column

oscillation described by Eq.(12) receiving the force described by Eq.(15) gains the following energy.

$$\int \frac{d\zeta}{dt} F dt = -\pi \epsilon_1 \epsilon_2 X^2 \cos(\phi_1 + \phi_2) \quad (16)$$

Since ϵ_1 and ϵ_2 are positive, energy is supplied to the oscillation when $\cos(\phi_1 + \phi_2) < 0$. In order to determine ϕ_1 , we need to examine jet behavior in a fluctuating pressure field.

6. Calculation of Jet Streakline

A plane jet of thickness b is issued from the inlet at $x=0$ and impinges on the free surface at $x=h$ as shown in Fig. 7. Although the free surface is a boundary through which no flow can penetrate, the turn at the surface is neglected here for simplicity. Disregarding the velocity profile of a thin stream, vertical and lateral velocity components are represented by mean values U and V , respectively. The lateral displacement of stream η can be calculated using the following equations⁽³⁾.

$$\eta(x, t) = \int_{t-\tau}^t (t-t') \frac{dV}{dt'} dt' \quad (17)$$

$$\tau(x) = \int_0^x \frac{dx'}{U(x')} \quad (18)$$

When the surface level ζ on the positive side ($y > 0$) oscillates alternately with the other ($y < 0$) as described in Eq.(12), there appears a pressure difference Δp in Eq.(13) across the jet. The mass element of the stream at x experiences a lateral acceleration given by

$$\frac{dV}{dt} = -\frac{\Delta p(t)}{\rho B(x)}, \quad (19)$$

where B is the representative thickness of the stream. If we know the representative values $U(x)$ and $B(x)$, we can calculate the streakline using a numerical method.

The actual jet has a velocity distribution in the lateral direction given as follows⁽⁴⁾.

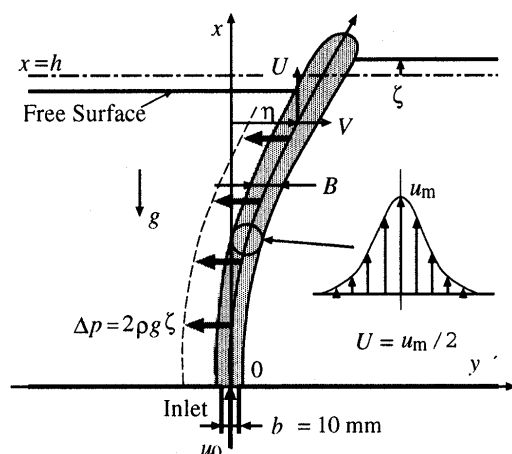


Fig. 7 Calculation model

$$u(x, y) = u_m(x) \operatorname{sech}^2 \left\{ \frac{4(y-\eta)}{B(x)} \right\}, \quad (20)$$

$$u_m(x) = \frac{1.2u_0}{\sqrt{a(x-x_p)/b}}, \quad (21)$$

$$B(x) = \frac{4a}{0.96}(x-x_p), \quad (22)$$

where u_0 is inlet velocity, u_m is velocity at the center, b is inlet width, $a=0.11$ is an experimental constant and $x_p = -0.41b/2a$ is pole position. The same profile is assumed in the upstream region for simplicity, although the developing velocity profile cannot be expressed by Eqs.(20)~(22) in reality. The jet width B satisfies the following equation.

$$B(x) = \int_{-\infty}^{\infty} \frac{u(x, y) dy}{U(x)} \quad (23)$$

When a jet receives a transverse force, particles at different distances from the jet center have different pathlines intersecting with each other. The mixing motion intensifies the turbulence, and there grows a disturbance propagating in the axial direction at a certain speed. The speed is roughly the same as the velocity where the velocity gradient is steepest. Thus we assume

$$U(x) = 0.5u_m(x). \quad (24)$$

Using Eqs.(17)~(24), we can calculate the path of jet by the Runge-Kutta method.

If the periodic time is infinitely long, the impinging point of jet on the surface shifts to the left when the water level on the right is high; η_h and ζ are in opposite phase as shown in Fig. 8(a). While the periodic time of column oscillation increases only in proportion to \sqrt{h} , the time required for jet to travel from the inlet to the surface increases in proportion to h . Therefore, the history of received force on the upstream path shows a stronger effect with increasing h , enlarging the phase lag of η_h behind $-\zeta$. In Fig. 8(d), the impinging point of jet on the surface shifts to the right when the water level on the right is high; η_h is nearly in phase with ζ .

7. Measurement of Jet Streakline

Since the calculation of streakline was based on the rough model, the results were compared with experimental results. The visualized streaklines of jet during nearly one cycle are shown in Fig. 9. The downstream jet displacement lagged behind that near the inlet, and the phase lag increased as the jet approached the surface. The swell position almost corresponds to the jet impinging point on the surface. The phase and the amplitude of jet displacement are quantitatively illustrated in Fig. 10 as well as those of swell position, where the phase lag ϕ is taken to be 0 at the jet inlet $x=0$. The jet centerline was determined assuming that the center was least contaminated by

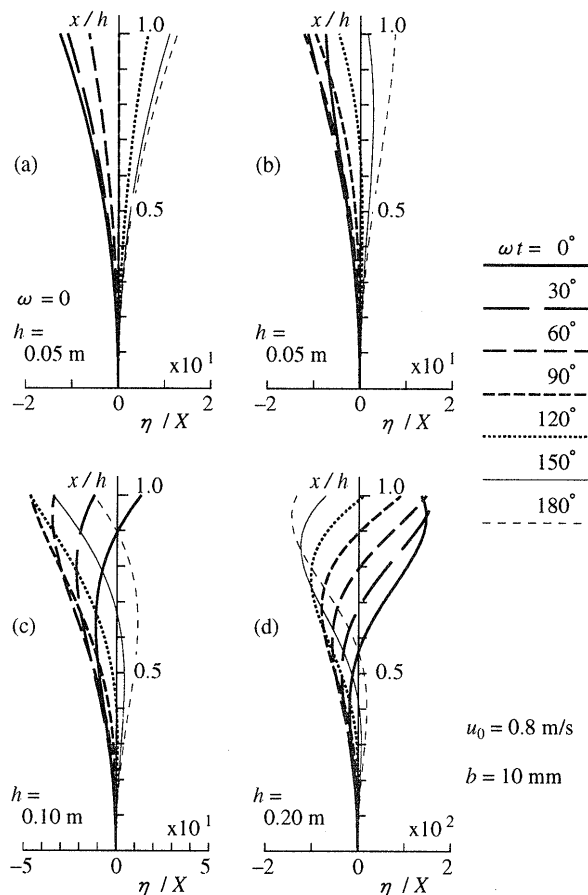


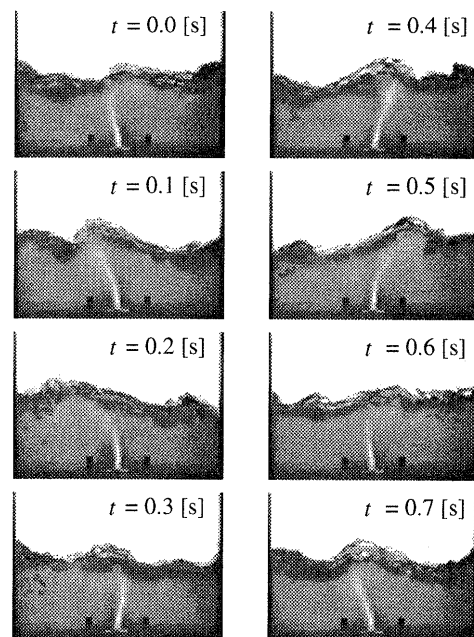
Fig. 8 Streaklines

ink in the surrounding water. In order to attain high accuracy, average behavior of the jet during several cycles was obtained using Fourier transformation. Both the amplitude and the phase lag increased with decreasing distance from the surface except in the neighborhood of the surface where intensive mixing with surrounding water lowered data reliability.

The calculated results are also shown in Fig. 10, where the amplitude is normalized in order to coincide with the experiment at $x = h/2$. Besides the agreement in the amplitude, which is natural because of normalization, the calculated phase agreed well with the measured one in the case of small h . However, the calculation with larger h gave a larger phase lag than the experiment. The main reason is that wave speed U in the experiment was higher than $0.5u_m$ when the tank was deep. A pair of steady convection currents was generated on both sides of the jet in the deep tank, which made the steepest gradient velocity higher than $0.5u_m$. If the existence of steady convection is taken into consideration, the agreement will be improved.

8. Oscillation Region

An examination of jet behavior in a fluctuating pressure field gave the dependence of ϕ_1 on h and u_0 .



$u_0 = 0.8 \text{ m/s}$ $h = 0.098 \text{ m}$ $b = 10 \text{ mm}$

Fig. 9 Visualized streaklines

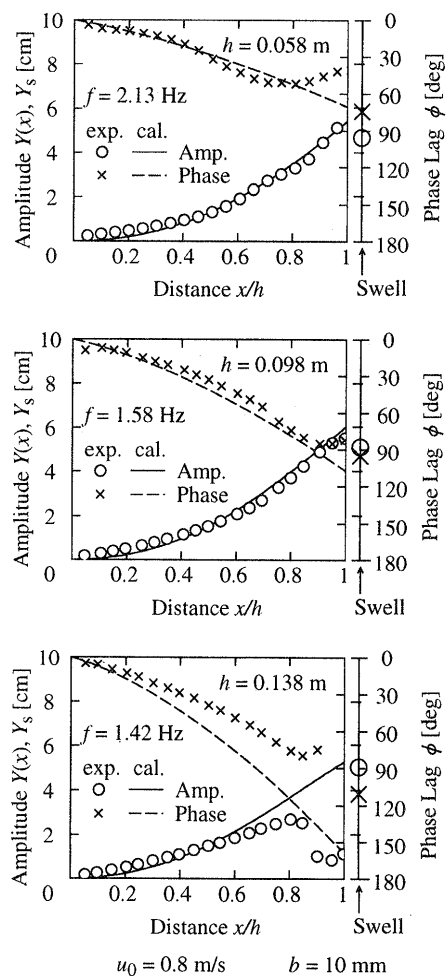


Fig. 10 Measured and calculated jet displacement

In order to obtain the dependence of ϕ_2 , we need to know the jet velocity at $x=h$. Substituting $x=h$ into Eq. (21), we obtain $u_h=u_m(h)$, the ordinate in Fig. 11. This value exceeds the inlet velocity u_0 when h is very small. Since u_h larger than u_0 is obviously meaningless, u_0 is used for u_h when $u_m(h)$ exceeds u_0 . The height of the swell is written by

$$h_s = \frac{u_h^2}{2g} \quad (25)$$

The abscissa of Fig. 11 is obtained from Eq. (25) using measured h_s . The calculated and measured values do not coincide completely, partly because Eq. (21) is a rough approximation and partly because the measurement of h_s is disturbed by fast recirculating flows in the small tank. Since the coincidence is fairly satisfactory, the calculated u_h is used in the following.

Substituting the calculated u_h into Eq. (25) and then into Eq. (1), the frequency is calculated. Using the frequency and the jet behavior calculation, the phase lag of the jet impinging point behind the water column oscillation is obtained as shown in Fig. 12. On the ordinate where $h=0$, the phase lag ϕ_1 is 0; ϕ_1

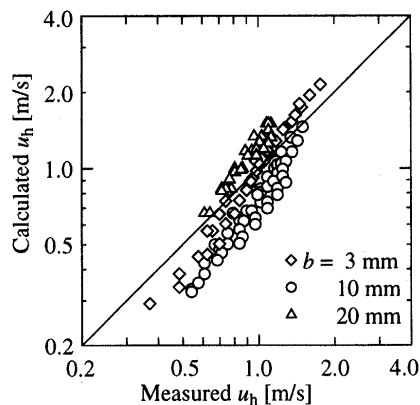


Fig. 11 Jet velocity on surface

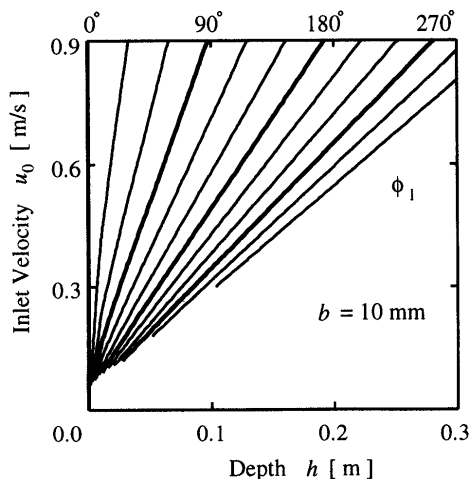


Fig. 12 Phase lag of jet impinging point η_h behind water column oscillation $-\zeta$

increases with increasing h/u_0 . The calculated value of ϕ_2 , the phase lag of unbalance generation behind the jet impingement, is shown in Fig. 13; ϕ_2 is 0 on the abscissa and increases with decreasing h/u_0 . On the ordinate where $h=0$, $\phi_2=\omega u_h/g=2$ because $\omega=\sqrt{2g/h_s}=2g/u_h$, which is larger than $\pi/2$ ($=90^\circ$). Figure 14 shows $\phi_1+\phi_2$, the total phase lag.

The condition $\cos(\phi_1+\phi_2)<0$ is always satisfied in the measured oscillation region as shown in Fig. 14. However, the oscillation is not necessarily induced in the region where $\cos(\phi_1+\phi_2)<0$ is satisfied. The oscillation increases when supplied energy exceeds dissipated energy. The amount of supplied energy is proportional not only to $-\cos(\phi_1+\phi_2)$ but also to ε_1 and ε_2 . Since ε_2 is proportional to the height of the swell, it decreases rapidly with increasing h/u_0 . The oscillation cannot increase near the boundary of $\phi_1+\phi_2<270^\circ$ because the supplied energy does not exceed the dissipated energy. The existence of swell

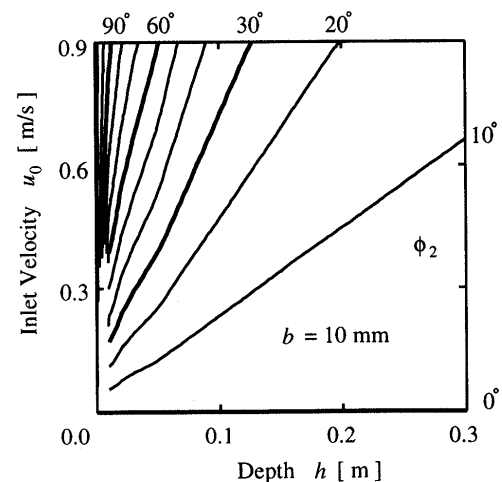


Fig. 13 Phase lag of imbalance generation q behind jet impingement η_h

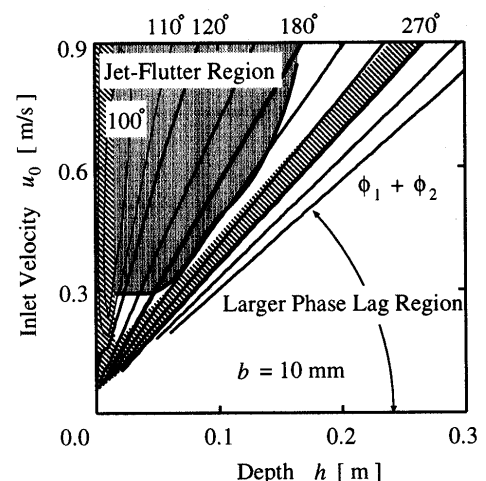


Fig. 14 Total phase lag $\phi_1+\phi_2$

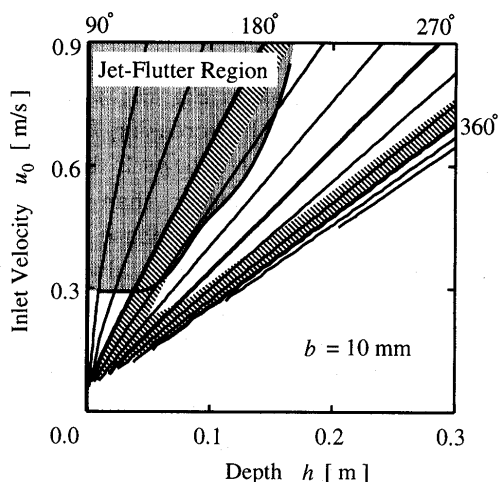


Fig. 15 Phase lag of force caused by momentum flux

is a necessary condition for the generation of jet-flutter, which is the outstanding characteristic of the phenomenon. The total phase lag $\phi_1 + \phi_2$ increases further with increasing h/u_0 and the condition $\cos(\phi_1 + \phi_2) < 0$ is satisfied again in regions near the abscissa. However, the oscillation is not likely to increase there because of small ε_2 .

While the above discussion is limited to the case of $b=10$ mm, the model explains the influence of the inlet width. A thin jet decelerates more rapidly than a thick jet. Therefore, the former ϕ_1 is larger than the latter when the inlet velocity is the same. The large ϕ_1 is compensated by a small ϕ_2 only partially. Thus the former needs a higher inlet velocity than the latter in order to satisfy the condition $\cos(\phi_1 + \phi_2) < 0$.

9. Comparison with Self-Induced Sloshing

Another type of oscillation, self-induced sloshing, occurs without formation of a surface swell. The energy is considered to be supplied by an influx of momentum caused by the fluttering motion of the jet⁽⁵⁾. In the following, it is examined whether jet-flutter can be caused by the same mechanism as self-induced sloshing or not. An apparent force F' acting in the area $y > 0$, i.e., increase in momentum in the area, is calculated as follows.

$$F' = \rho \int_0^h u_m \frac{\partial \eta}{\partial t} dx, \quad (26)$$

where jet displacement η is assumed to be small compared with jet thickness. Energy is supplied to the oscillation in the case F' is $180^\circ \sim 360^\circ$ behind ζ . Figure 15 shows the calculated phase lag of F' behind ζ , which takes a value between 180° and 360° in the fan-shaped region apart from the ordinate. The oscillation was observed in the experiment in case of small h/u_0 where the phase lag was less than 180° , and the force F' did not supply energy to the oscillation. The influx of momentum caused by fluttering motion

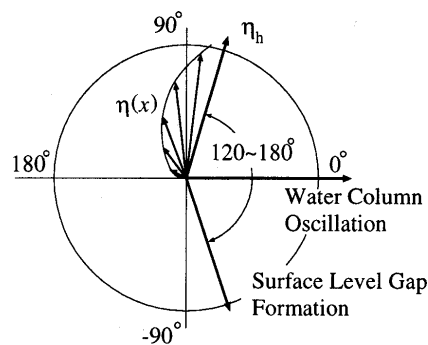


Fig. 16 Phase of variables

of a jet was not the cause of jet-flutter, on the contrary, it damped the oscillation. When jet-flutter grows, energy supply by F in Eq. (15) exceeds energy dissipated by F' which is usually smaller than F .

10. Phase Relations

According to the jet behavior calculation, water column oscillation ζ and jet displacement $\eta(0)$, η at $x=0$, are in opposite phase. If we could measure the variation of ζ , this relation would be experimentally confirmed. However, superimposition of traveling waves on the surface made it difficult to measure the water level difference across the jet which governs the lateral displacement. Using pressure taps bored through the bottom plate at a distance of 40 mm from the jet axis, the pressure difference Δp was measured. The data of Δp had higher harmonics, and the amplitude of fundamental component varied irregularly due to the effect of traveling waves. Taking the standard phase of $\eta(0)$ to be 180° , the phase of Δp was about 30° , and not 0° . The cause of this discrepancy was not clear; the error might have appeared because of poor measurement methods, or the measured Δp might not represent the pressure difference governing the jet behavior. In the following, we assume that ζ is 180° ahead of $\eta(0)$ and take the phase of ζ to be 0° . The typical phase of η is shown in Fig. 16. The jet displacement η_h , η at $x=h$, oscillated about 90° ahead of ζ . The formation of surface level gap oscillated about $120^\circ \sim 180^\circ$, $\omega u_h/g$ added to 90° , behind η_h as can be seen in Eqs. (6) and (10). The level gap formation was $0^\circ \sim 180^\circ$ behind the column oscillation; thus, energy was supplied to the oscillation.

11. Conclusion

A model was proposed that explained two major characteristics of jet-flutter: the frequency corresponds to that of water column oscillation in a partitioned tank with the same water depth, and the oscillating region had a wide range above a certain velocity limit determined by the water depth. The

oscillation of a swell-making jet was revealed to cause apparent water column oscillation. A model was proposed to explain the energy supply mechanism, in which jet behavior was calculated by simplified method using a representative jet width and representative axial and transverse components of jet velocity. The calculated oscillation region agreed well with the experimental one, which supported the validity of the model.

References

- (1) Fukaya, M., Okamoto, K., Madarame, H. and Iida, M., Effects of Tank Geometries on Self-Induced Sloshing Caused by Upward Plane Jet, Proc. Asia-Pacific Vibration Conference '93 (APVC'93), Kitakyushu, (1993), p. 271-276.
- (2) Madarame, H., Iida, M., Okamoto, K. and Fukaya, M., Jet-Flutter: Self-Induced Oscillation of Upward Plane Jet Impinging on Free Surface, Proc. Asia-Pacific Vibration Conference '93 (APVC'93), Kitakyushu, (1993), p. 265-270.
- (3) Nyborg, W. L., Self-Maintained Oscillations of the Jet in a Jet-Edge System I, J. Acoust. Soc. Am., Vol. 26, No. 2 (1954), p. 174-182.
- (4) Abramovich, G. N., The Theory of Turbulent Jets, (1963) M. I. T. Press.
- (5) Fukaya, M., Madarame, H. and Okamoto, K., Growth Mechanism of Self-Induced Sloshing Caused by Vertical Plane Jet, Proc. Int. Conf. Nuclear Engrg. (ICONE-4), (1996), Vol. 1, p. 781-787.